

REPORT DOCUMENTATION PAGE			Form Approved OMB NO. 0704-0188		
<p>The public reporting burden for this collection of information is estimated to average 1 hour per response, including the time for reviewing instructions, searching existing data sources, gathering and maintaining the data needed, and completing and reviewing the collection of information. Send comments regarding this burden estimate or any other aspect of this collection of information, including suggestions for reducing this burden, to Washington Headquarters Services, Directorate for Information Operations and Reports, 1215 Jefferson Davis Highway, Suite 1204, Arlington VA, 22202-4302. Respondents should be aware that notwithstanding any other provision of law, no person shall be subject to any penalty for failing to comply with a collection of information if it does not display a currently valid OMB control number.</p> <p>PLEASE DO NOT RETURN YOUR FORM TO THE ABOVE ADDRESS.</p>					
1. REPORT DATE (DD-MM-YYYY)		2. REPORT TYPE New Reprint		3. DATES COVERED (From - To) -	
4. TITLE AND SUBTITLE Chemical Warfare Agent Surface Adsorption: Hydrogen Bonding of Sarin and Soman to Amorphous Silica			5a. CONTRACT NUMBER W911NF-09-1-0150		
			5b. GRANT NUMBER		
			5c. PROGRAM ELEMENT NUMBER 611102		
6. AUTHORS Erin Durke Davis, Wesley O. Gordon, Amanda R. Wilmsmeyer, Diego Troya, John R. Morris			5d. PROJECT NUMBER		
			5e. TASK NUMBER		
			5f. WORK UNIT NUMBER		
7. PERFORMING ORGANIZATION NAMES AND ADDRESSES Virginia Polytechnic Institute & State Univ North End Center, Suite 4200 300 Turner Street, NW Blacksburg, VA 24061 -0001			8. PERFORMING ORGANIZATION REPORT NUMBER		
9. SPONSORING/MONITORING AGENCY NAME(S) AND ADDRESS (ES) U.S. Army Research Office P.O. Box 12211 Research Triangle Park, NC 27709-2211			10. SPONSOR/MONITOR'S ACRONYM(S) ARO		
			11. SPONSOR/MONITOR'S REPORT NUMBER(S) 55374-CH.18		
12. DISTRIBUTION AVAILABILITY STATEMENT Approved for public release; distribution is unlimited.					
13. SUPPLEMENTARY NOTES The views, opinions and/or findings contained in this report are those of the author(s) and should not be construed as an official Department of the Army position, policy or decision, unless so designated by other documentation.					
14. ABSTRACT Sarin and soman are warfare nerve agents that represent some of the most toxic compounds ever synthesized. The extreme risk in handling such molecules has, until now, precluded detailed research into the surface chemistry of agents. We have developed a surface science approach to explore the fundamental nature of hydrogen bonding forces between these agents and a hydroxylated surface. Infrared spectroscopy revealed that both agents adsorb to amorphous silica through the formation of surprisingly strong hydrogen-bonding interactions with primarily isolated silanol groups (SiOH). Comparisons with previous theoretical results reveal that this bonding occurs almost					
15. SUBJECT TERMS Sarin, Soman, DIMETHYL METHYLPHOSPHONATE; BINDING-ENERGIES; DECOMPOSITION; SiO2					
16. SECURITY CLASSIFICATION OF:			17. LIMITATION OF ABSTRACT UU	15. NUMBER OF PAGES	19a. NAME OF RESPONSIBLE PERSON John Morris
a. REPORT UU	b. ABSTRACT UU	c. THIS PAGE UU			19b. TELEPHONE NUMBER 540-231-2472

## **Report Title**

Chemical Warfare Agent Surface Adsorption: Hydrogen Bonding of Sarin and Soman to Amorphous Silica

### **ABSTRACT**

Sarin and soman are warfare nerve agents that represent some of the most toxic compounds ever synthesized. The extreme risk in handling such molecules has, until now, precluded detailed research into the surface chemistry of agents. We have developed a surface science approach to explore the fundamental nature of hydrogen bonding forces between these agents and a hydroxylated surface. Infrared spectroscopy revealed that both agents adsorb to amorphous silica through the formation of surprisingly strong hydrogen-bonding interactions with primarily isolated silanol groups (SiOH). Comparisons with previous theoretical results reveal that this bonding occurs almost exclusively through the phosphoryl oxygen (P=O) of the agent. Temperature-programmed desorption experiments determined that the activation energy for hydrogen bond rupture and desorption of sarin and soman was 50 +/- 2 and 52 +/- 2 kJ/mol, respectively. Together with results from previous studies involving other phosphoryl-containing molecules, we have constructed a detailed understanding of the structure-function relationship for nerve agent hydrogen bonding at the gas-surface interface.

---

**REPORT DOCUMENTATION PAGE (SF298)**  
**(Continuation Sheet)**

---

Continuation for Block 13

ARO Report Number 55374.18-CH  
Chemical Warfare Agent Surface Adsorption: Hy...

Block 13: Supplementary Note

© 2014 . Published in The Journal of Physical Chemistry Letters, Vol. 5 (8) (2014), (5 (8)). DoD Components reserve a royalty-free, nonexclusive and irrevocable right to reproduce, publish, or otherwise use the work for Federal purposes, and to authorize others to do so (DODGARS §32.36). The views, opinions and/or findings contained in this report are those of the author(s) and should not be construed as an official Department of the Army position, policy or decision, unless so designated by other documentation.

Approved for public release; distribution is unlimited.

# Chemical Warfare Agent Surface Adsorption: Hydrogen Bonding of Sarin and Soman to Amorphous Silica

Erin Durke Davis,<sup>†</sup> Wesley O. Gordon,<sup>‡</sup> Amanda R. Wilmsmeyer,<sup>§</sup> Diego Troya,<sup>§</sup> and John R. Morris<sup>\*,§</sup>

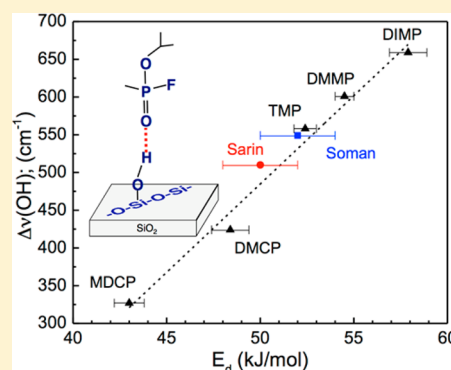
<sup>†</sup>EXCET, Inc., 8001 Braddock Road, Suite 303, Springfield, Virginia 22151, United States

<sup>‡</sup>Research and Technology Directorate, Edgewood Chemical Biological Center, Edgewood, Maryland 21010, United States

<sup>§</sup>Department of Chemistry, Virginia Tech, Blacksburg, Virginia 24061, United States

**ABSTRACT:** Sarin and soman are warfare nerve agents that represent some of the most toxic compounds ever synthesized. The extreme risk in handling such molecules has, until now, precluded detailed research into the surface chemistry of agents. We have developed a surface science approach to explore the fundamental nature of hydrogen bonding forces between these agents and a hydroxylated surface. Infrared spectroscopy revealed that both agents adsorb to amorphous silica through the formation of surprisingly strong hydrogen-bonding interactions with primarily isolated silanol groups (SiOH). Comparisons with previous theoretical results reveal that this bonding occurs almost exclusively through the phosphoryl oxygen (P=O) of the agent. Temperature-programmed desorption experiments determined that the activation energy for hydrogen bond rupture and desorption of sarin and soman was  $50 \pm 2$  and  $52 \pm 2$  kJ/mol, respectively. Together with results from previous studies involving other phosphoryl-containing molecules, we have constructed a detailed understanding of the structure–function relationship for nerve agent hydrogen bonding at the gas–surface interface.

**SECTION:** Surfaces, Interfaces, Porous Materials, and Catalysis



The threat of chemical warfare agents (CWAs), particularly the nerve agents sarin (*RS*-propan-2-yl methylphosphonofluoridate, GB) and soman (3,3-dimethylbutan-2-yl methylphosphonofluoridate, GD), to the global community has motivated researchers to explore new methods for the detection of agents, the destruction of existing stockpiles, and the decontamination of affected areas, with the ultimate goal of providing effective protection of military and civilian personnel. Critical to the development of strategies for combating the threat of CWAs is a detailed understanding of agent–surface chemistry. However, scientists have largely been restricted to conducting experiments with less toxic analogues (often referred to as simulants) of the actual agents. These simulants (Figure 1) contain the central phosphoryl ester of the actual agents, but they lack the structure and key chemical functionality of the agents, which makes the prediction of agent–surface chemistry tenuous. For example, recent work has shown that dimethyl methylphosphonate (DMMP), the most commonly employed simulant, binds to the surface of hydrophilic silica much more strongly than dimethyl chlorophosphate (DMCP),<sup>1</sup> which implies that a phosphorus–halogen bond, such as that found in sarin, may affect the surface chemistry of the agent in ways that cannot be predicted by studying the simulant alone. In fact, calculations suggest that the electron-withdrawing character of the fluorine group in sarin has a major impact on its interfacial hydrogen-bonding strength.<sup>2</sup> We have therefore developed an ultrahigh vacuum (UHV) surface science approach to the study of agent–surface

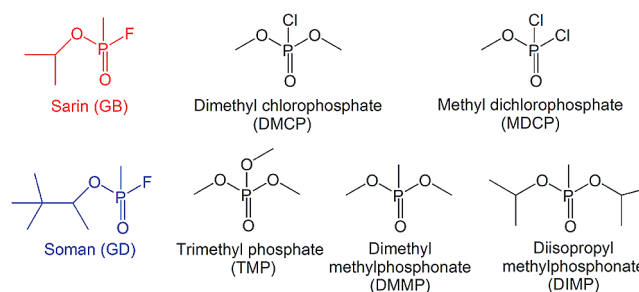


**Figure 1.** The structures of the CWAs sarin (red) and soman (blue) and five of the most common simulants (black) used to help predict agent chemistry.

chemistry. Here, we present direct studies of the mechanisms and energetics that govern hydrogen-bonding forces when sarin and soman adsorb to one of the most abundant materials found on Earth, silica. In addition to the relevance of silica surface chemistry to many areas of environmental science, the material serves as an excellent test system for exploration of the fundamental nature of molecule–surface hydrogen bond forces, which play a critical role throughout chemistry and control the uptake and residence times of molecules on the surface of a variety of materials from coatings to oxides.

**Received:** February 20, 2014

**Accepted:** March 17, 2014

**Published:** March 17, 2014

Experiments were performed in an UHV surface science instrument recently developed for the study of CWAs and other highly toxic compounds (see the Experimental Methods section). Located in a laboratory at the Aberdeen Proving Grounds, the instrument (Figure S) enables measurements of surface adsorption through infrared (IR) spectroscopy and X-ray photoelectron spectroscopy (XPS), while gas-phase products are monitored via a quadrupole mass spectrometer.<sup>3</sup> Particulate silica surface samples were prepared by dispersing silica (200 m<sup>2</sup>/g, Aerosil fumed silica with a 12 nm average particle diameter) from a solution of isopropanol onto a reflective Au substrate, which served as an inert support and reflective mirror for performing IR spectroscopy of the silica during agent exposure. Once prepared, the surface samples were installed via a load-lock mechanism that couples the main chamber sample holder to a small transfer chamber located within the confines of a CWA-certified surety fume hood. Within the main chamber, the sample was mounted on a molybdenum platen, which can be heated via a tungsten filament and cooled with liquid nitrogen. Prior to each experiment, the sample was cleaned by thermal annealing to 700 K before cooling the sample to 200 K, where dosing was conducted. IR and XPS measurements were used to verify that the surface of the silica was clean to less than 0.1% coverage of organic contaminants. In addition to sample cleaning, heating to 700 K produces a partially dehydroxylated surface. The OH coverage for our sample is estimated to be 2 OH/nm<sup>2</sup>, which is typical for particulate silica under these sample preparation conditions.<sup>4–6</sup> Chemical Agent Standard Analytical Reference Material (CASARM)-grade sarin (98.7% by NMR) and soman (96.0% by NMR) were used for all experiments. (CAUTION: Experiments performed with ultratoxic CWAs require extreme care, highly trained operators, and a secure government-regulated facility.) Prior to experiments, the gas manifold and dosing lines were heated, under vacuum, to 100 °C to minimize water contamination. A stainless steel reservoir containing 30  $\mu$ L of agent was then connected to the manifold, and the sample was purified via three freeze–pump–thaw cycles. Within the main UHV chamber, controlled exposure of the surface to the agent of interest was achieved through a directional doser positioned 2 cm from the center of the silica sample. Agent uptake was monitored via IR spectroscopy, performed with a Bruker Vertex 80v FTIR spectrometer coupled to the UHV chamber. Each spectrum was the average of 100 scans collected at a 2 cm<sup>−1</sup> resolution with a 6 mm aperture and 20 kHz scanning velocity. The spectra presented here are difference spectra, where the reference spectrum is that of the thermally treated silica.

Previous studies have shown that the uptake of organophosphonate simulants on the surface of silica occurs through the formation of hydrogen bonds to free silanol groups.<sup>1,7–10</sup> The IR spectral signature for hydrogen bonding between adsorbates and silica is a broad SiO–H stretching mode that appears red-shifted from its original frequency. Figure 2 shows IR spectra of the partially dehydroxylated SiO<sub>2</sub> particles during adsorption of either sarin (Figure 2A) or soman (Figure 2B). The data reveal a significant change in the original free SiO–H vibrational band, while energies of other modes associated with the adsorbates are largely independent of coverage. These observations indicate that adsorption indeed occurs through strong interactions with surface hydroxyl groups and that the geometry of the adsorbates is independent of coverage within the low-coverage regime employed in this work.

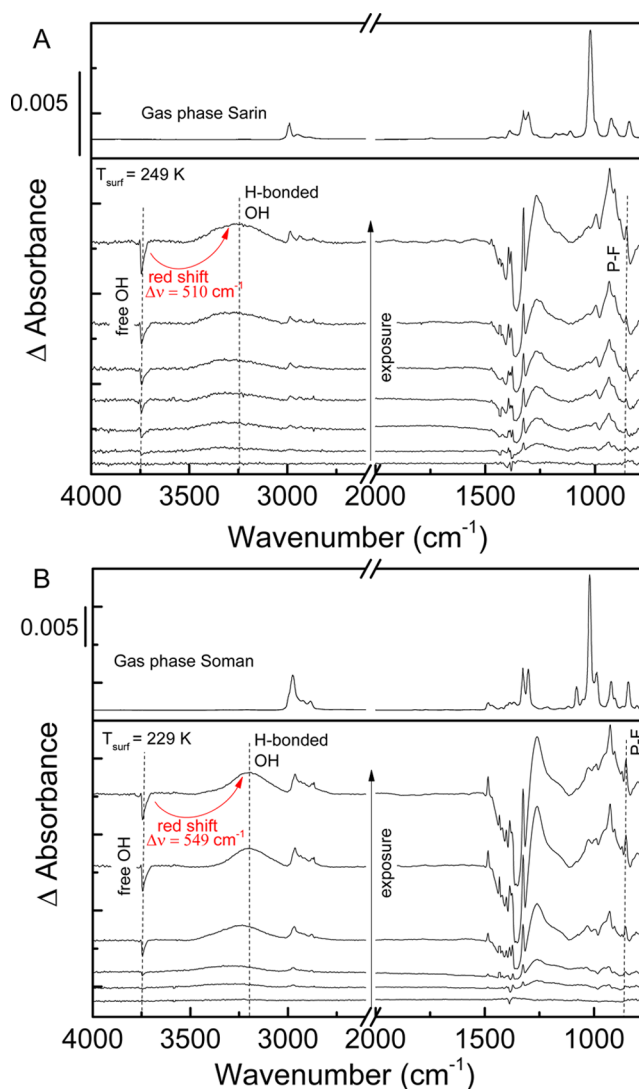


**Figure 2.** (A) Difference IR spectra of amorphous silica exposed to gas-phase sarin (bottom) and IR spectra for gas-phase sarin (top). The spectra displayed in the lower portion of the graph show the uptake of sarin during exposure. (B) The top panel shows the IR spectrum for gas-phase soman, and the bottom panel shows spectra collected during exposure of silica to soman. The IR peaks are assigned to particular local modes, as indicated in Table 1. It should be noted that definitive assignment of features, especially broad peaks, in the region below  $\sim 1400$  cm<sup>−1</sup> cannot be made because they are obscured by high absorbance of the bulk modes of silica (see Figure 6), and changes in this region are due largely to the change in index of the refraction of the underlying silica upon adsorption.

The IR spectra for the two agents are very similar, reflecting the similarities in their molecular structure and surface bonding configurations. Specifically, Table 1 shows that the low-energy bending and deformation modes are within  $\sim 10$  cm<sup>−1</sup> of each other for the two adsorbates. In addition, the higher-energy C–H symmetric and asymmetric modes nearly overlap in wavenumber. Finally, the primary IR modes associated with hydrogen-bonded surface hydroxyls differ by only  $\sim 40$  cm<sup>−1</sup>, which suggests that sarin and soman may have similar binding structures, energetics, and overall mechanisms.

For both adsorbates, the agent–surface hydrogen bond appears to be dominated by interactions between the surface SiOH groups and the sp<sup>2</sup> oxygen (P=O) of the adsorbates.

**Table 1.** Assignments of the IR Peaks for Sarin and Soman in the Gas Phase and Adsorbed on Silica

mode	sarin		soman	
	gas <sup>a</sup>	ads.	gas <sup>a</sup>	ads.
Si(O–H) <sub>free</sub>	<i>b</i>	3745	<i>b</i>	3745
Si(O–H) <sub>bonded</sub>	<i>b</i>	3235	<i>b</i>	3196
$\nu_a(\text{CH}_3\text{C})$	2990	2994	2975	2972
$\nu_s(\text{CH}_3\text{C})$	2949	2934	2922	2937
$\nu(\text{CH})$	2890	2881	2878	2878
$\delta_s(\text{CH}_3)$	<i>b</i>	<i>b</i>	1485	1484
$\delta_a(\text{CH}_3)$	<i>b</i>	<i>b</i>	1466	1467
$\delta_a(\text{CH}_3\text{P})$	1424	1422	1424	1419
$\delta_a(\text{CH}_3\text{C})$	1392	1470	<i>b</i>	<i>b</i>
$\delta_a(\text{CH}_3\text{C})$	1387	1461	<i>b</i>	<i>b</i>
$\delta_s(\text{CH}_3\text{C})$	1392	1393	<i>b</i>	<i>b</i>
$\delta_s(\text{CH}_3\text{C})$	1387	1381	<i>b</i>	<i>b</i>
$\delta_s(\text{CH}_3\text{P})$	1326	1325	1326	1324
$\nu(\text{P=O})$	1303	<i>e</i>	1301	<i>e</i>
$\delta_a(\text{CH}_3\text{C})$	1387	1461	<i>b</i>	<i>b</i>
$\rho_a(\text{CH}_3\text{C})$	1148	1147		
$\nu(\text{C–OP})$	1022	1023	1021	1029
CCC bend			991	1000
$\rho_a(\text{CH}_3)$	927	931	922	927
$\rho_a(\text{CH}_3)$	910	910	905	905 <sup>c</sup>
$\nu_s(\text{CCC})$	887 <sup>d</sup>	886 <sup>d</sup>	869 <sup>d</sup>	871 <sup>d</sup>
$\nu(\text{P–F})$	844	846	803	825
$\nu(\text{P–C})$			752	753

<sup>a</sup>See ref 11. <sup>b</sup>Indicates that modes are not present in the molecule.<sup>c</sup>May correspond to a CCC bend. <sup>d</sup>See ref 12. <sup>e</sup>Obscured by bulk SiO<sub>2</sub> modes.

This conclusion is based primarily on previous theoretical studies,<sup>2</sup> which have shown that the largest surface binding energy occurs for P=O...HOSi interactions. For example, the hydrogen bonding energies for sarin to silanol groups were reported to be approximately 4 kcal/mol greater when bonding through the O(sp<sup>2</sup>) than those through the O(sp<sup>3</sup>) or through the F groups surrounding the molecule.

Upon hydrogen bond formation, charge transfer from the adsorbate to the hydrogen bond acceptor partially populates the  $\sigma^*$  orbital of the OH group to weaken this bond. This change in the character of the O–H bond is reflected in the red shift of the vibrational frequency of this mode. Furthermore, a distribution of bonding configurations and the reduced lifetime of the O–H stretching mode, as the vibration couples to other modes of the adsorbate, contribute to a significant broadening of this peak.

Recent work has suggested that the shift in the surface SiO–H stretching frequency is strongly correlated to the strength of the hydrogen bond for like molecules that adsorb to silica through a central phosphoryl group.<sup>7</sup> In particular, we have shown that the desorption energies from silica (for the compounds highlighted in Figure 1) scale linearly with the change in frequency of the SiO–H mode.<sup>7</sup> Therefore, one might predict, on the basis of the IR spectra in Figure 2, that sarin and soman have similar binding energies. We have tested this hypothesis through quantitative determination of the desorption energy for these two molecules.

The experimental temperature-programmed desorption (TPD) data, which display the rate of desorption for sarin and soman as a function of surface temperature, are shown in Figure 3A and C. In these studies, a doubly differentially

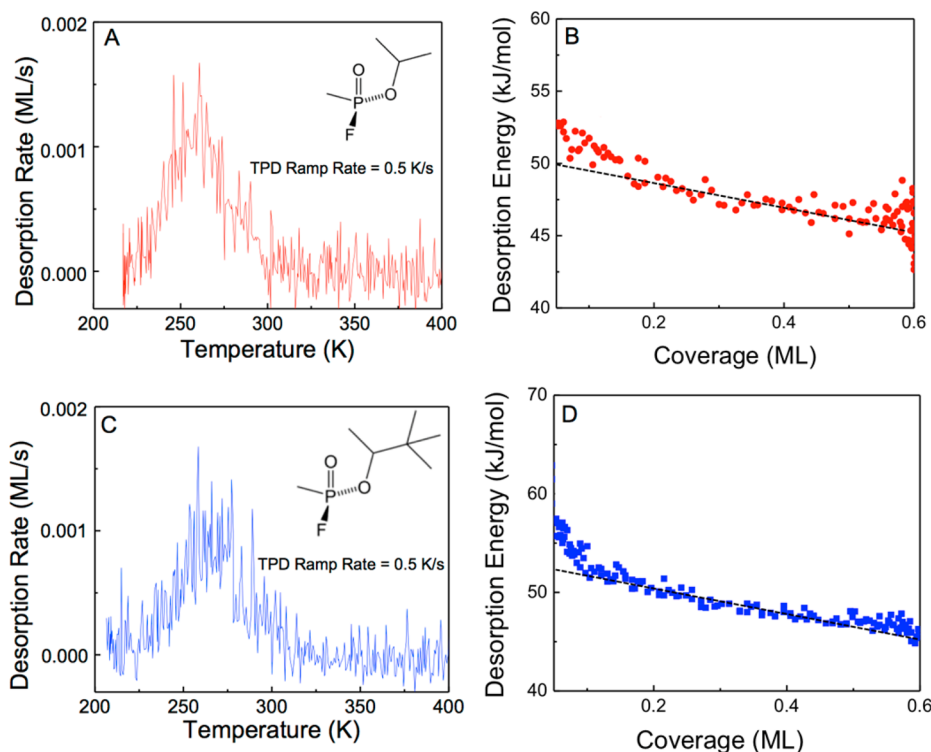


**Figure 3.** (A) TPD data collected for the desorption of sarin from amorphous silica. After exposure of the silica to gas-phase sarin, the surface temperature was ramped at a rate of 0.5 K/s. (B) The desorption energy of sarin from silica as a function of surface coverage determined by inversion of the Polanyi–Wigner equation. (C) TPD data for soman desorbing from amorphous silica. The data in panel C was analyzed via inversion of the Polanyi–Wigner equation to provide the coverage-dependent desorption energy (D).



pumped mass spectrometer was used to monitor the desorption rate for each molecule during a linear thermal ramp of the surface. We note that the mass spectrometric cracking patterns for sarin and soman molecules as they desorbed from the surface were identical to those of the parent molecules, which indicates that molecular dissociation is very limited on the silica surface. This conclusion is supported by the IR data of Figure 2, which shows spectroscopic evidence for molecular adsorption.

Determination of the desorption energy ( $E_d$ ) from the TPD data was achieved through inversion of the Polanyi–Wigner equation

$$-\frac{d\Theta}{dt}(\Theta, T_s) = \nu(\Theta, T_s)e^{-E_d(\Theta)/k_B T_s}\Theta^n \quad (1)$$

In this equation,  $\nu$  is the preexponential factor,  $\Theta$  is the coverage,  $T_s$  is the surface temperature,  $k_B$  is the Boltzmann constant, and  $n$  is the order for desorption (simple molecular desorption is expected to be first order,  $n = 1$ ).<sup>11</sup> The inversion analysis is accomplished by solving the above equation for the coverage-dependent desorption energy

$$E_d(\Theta) = -k_B T_s \ln\left(-\frac{d\Theta/dt}{\nu\Theta}\right) \quad (2)$$

For this work, we used a pre-exponential factor determined for the desorption of the simulant DMMP from the silica sample,  $\nu = 4.0 \times 10^{6 \pm 0.8} \text{ s}^{-1}$ .<sup>1</sup> Although safety constraints precluded us from performing the types of repeated exposure-dependent TPD studies required for determination of a unique pre-exponential factor for the agents, the pre-exponential for DMMP has been shown to accurately model the TPD data for all of the simulants highlighted in Figure 1.<sup>7</sup> Close agreement of the agent data with previously observed trends in the desorption energy for the simulants, as described below, helps to justify our use of the pre-exponential factor for DMMP in the current TPD analysis.

The  $E_d(\theta)$  results (Figure 3B and D) from inversion of the TPD data produce a range of binding energies, well above 45 kJ/mol, for both agents. In fact, the desorption energy for soman (blue) approaches 60 kJ/mol at the lowest coverages. The high activation energies of desorption found in this work exceed typical hydrogen bond strengths; however, the energetics are consistent with recent work by a number of groups that have performed electronic structure calculations of many agents and simulants on the surface of silica.<sup>8,9,12</sup> They are also consistent with calorimetric measurements of the heats of adsorption for sarin on silica.<sup>8</sup> The high hydrogen bond energy appears to be driven by the significant electron density surrounding the  $\text{sp}^2$  oxygen atom of the agents. Even with the strongly electron withdrawing fluorine substituent on the molecules, the charge on the oxygen may be as high as  $-0.6 e$ , where  $e$  is the charge of 1 electron, as determined from electronic structure calculations.<sup>2</sup> The significant charge on the oxygen creates large electrostatic interactions with the polar surface hydroxyl groups and facilitates partial charge transfer (as evidenced by the large red shift of the  $\text{SiO}-\text{H}$  stretch) to produce strong hydrogen bonding forces (as evidenced by the TPD measurements).

Overall, the data of Figure 3 show that the molecule–surface interactions are weakest for the highest surface coverages ( $\sim 45$  kJ/mol for sarin,  $\sim 47$  kJ/mol for soman) but become stronger, by  $\sim 5$  kJ/mol, as the coverage decreases. This observation indicates that, under these experimental conditions, the

molecules readily diffuse to the most stable unoccupied sites that produce the tightest binding. In this way, the increase in energy suggests that there are a variety of surface sites or configurations, each leading to slightly different energies. Alternatively, there may be small repulsive interactions between the adsorbates, the extent of which depends on coverage. The strongest binding sites, responsible for the upturn in the  $E_d$  curve for soman at low coverage, may be defect sites or areas where many hydroxyl groups contribute simultaneously to the adsorption. The binding energy for isolated hydroxyl groups in defect-free regions of the surface can be estimated by extrapolating the linear portion of the energy distribution curves to zero coverage (dashed line in Figures 3B and D). This analysis indicates that the energy for desorption of sarin from isolated  $\text{SiOH}$  groups is  $50 \pm 2$  kJ/mol and that of soman is  $52 \pm 2$  kJ/mol.

Recently, Wilmsmeyer et al.<sup>1,7</sup> explored the relationship between molecular functionality and interfacial organophosphate hydrogen bonding at the gas–surface interface of silica. In their studies, the coverage-dependent desorption energies for the CWA simulants DMMP, DIMP, DMCP, MDCP, and TMP were measured in conjunction with IR spectroscopic studies of the adsorbed species.<sup>1,7</sup> The reported  $E_d$  values were  $43.0 \pm 0.8$  (MDCP),  $48.4 \pm 1.0$  (DMCP),  $52.4 \pm 0.6$  (TMP),  $54.5 \pm 0.5$  (DMMP), and  $57.9 \pm 1$  (DIMP) kJ/mol. The experimental measurements, together with electronic structure calculations, revealed that the desorption energy from an isolated silanol group is directly related to the charge on the  $\text{sp}^2$  oxygen atom of the simulant, thus demonstrating that hydrogen bond formation occurred exclusively through the central phosphoryl group. The other substituents affect the charge on the  $\text{sp}^2$  oxygen, but they are not directly involved in hydrogen bond formation. That is, the binding energy decreases with the electron-withdrawing ability of the surrounding functional groups. For example, the chlorine substituents of MDCP significantly decrease the electron density of the phosphoryl moiety, thus weakening the interfacial hydrogen bond. Substitution of the chlorine with a methyl or large isopropoxy group (e.g., DIMP) results in stronger binding with the surface. Similar results were reported in the recent computational studies by Troya et al.,<sup>2</sup> in which they demonstrated that the fluorine substituent in sarin reduced the electron density of the  $\text{sp}^2$  oxygen but that this effect was largely countered by the isopropoxy group of the molecule, which accounted for computed binding energies similar to those of the most common simulants. The net effect of the halogen atoms appears to be that of withdrawing electron density from the  $\text{sp}^2$  oxygen, which is the most important factor in determining the strength of adsorption and the activation energy for desorption.

The relationship between the energy for desorption and the change in the vibrational frequency of the surface  $\text{SiO}-\text{H}$  mode upon adsorption has been shown to be remarkably linear for the series of simulants presented in Figure 1. With the results reported above, we find that the actual agents agree very well with this trend. Figure 4 shows the previously published relationship between desorption energy and  $\text{SiO}-\text{H}$  vibrational frequency for the simulants,<sup>7,13</sup> along with the addition of two key data points for the agents. This relationship demonstrates that the binding mechanism for each molecule is similar, with the dominant contribution to the strength of the hydrogen bond being interactions between the  $\text{sp}^2$  oxygen of the adsorbates and the  $\text{SiOH}$  groups of the surface. Further, the simulant that most closely mimics the energetics of the agents

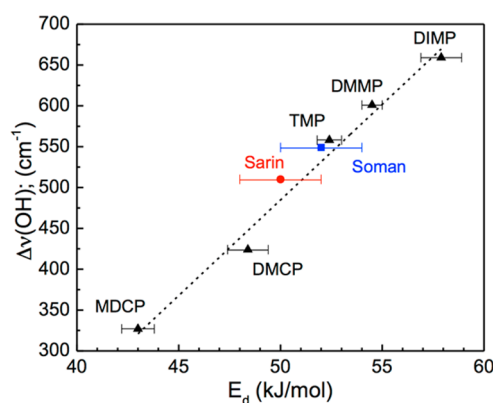


**Figure 4.** Plot of the change in wavenumber of the SiO–H stretching mode ( $\Delta\nu$ ) and the desorption energy ( $E_d$ ) for the agents and simulants.

is TMP. Interestingly, the strong electron-withdrawing character of the fluorine atom on the agents does not lead to weak hydrogen-bonding interactions because this effect appears to be balanced by the charge-donating character of the oxygen-containing substituents.

This correlation between nerve agents and the most common simulants will better enable researchers to choose the most appropriate simulants as well as provide critical benchmarks for computational studies of agents where hydrogen-bonding interactions play a role in the overall chemistry. Most importantly, the results provide fundamental insight into the structure–function relationship in hydrogen-bond formation at the gas–surface interface that extends our understanding of this critical chemical interaction.

## EXPERIMENTAL METHODS

The custom multifunctional UHV chamber specifically designed to safely allow experiments with ultratoxic chemicals used for this work is described in a previous article<sup>3</sup> and is depicted schematically in Figure 5. The chamber combines multiple vacuum dosing methods for liquids and vapors and the ability to perform surface-sensitive IR spectroscopy and XPS as well as mass spectrometry (MS). The instrument is built around a 23 L UHV chamber constructed out of 316L stainless steel with all ports equipped with con-flat flanges (Kurt J. Lesker Company). The chamber is evacuated with a 2200 L/s magnetically levitated turbomolecular pump (A2200C, Edwards Vacuum). This pump is backed by a scroll pump (XDS-35, Edwards Vacuum).

Samples are introduced into the chamber via a high-vacuum load-lock system that is coupled to the chamber through a 6 in. gate valve. Samples are mounted onto a molybdenum platen, which is in turn secured onto the linear transfer arm via a spring-loaded fork (customized STLC transfer system, Thermionics, Inc.). Once evacuated, the load-lock gate valve is opened to enable transfer of the sample platen on to the manipulator (Thermionics, Inc.), which allows travel in the X, Y, and Z dimensions, full 360° of rotation, and tilt in the X and Y planes. This enables the sample to be positioned as required for the experiment. The sample platen features a transferrable type K thermocouple, which is spot-welded to the surface.

Sarin and soman were dosed as a neat vapor using a multivalved stainless steel high-vacuum manifold. The entire path of the manifold was evacuated and heated to 100 °C prior to each experiment to eliminate water and other contaminants.

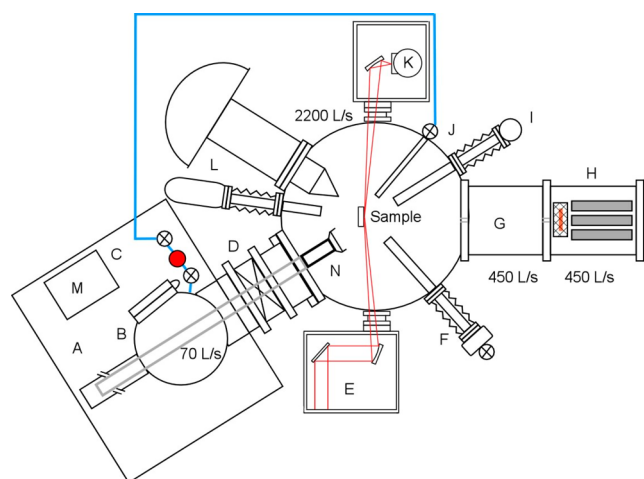


**Figure 5.** Schematic (not to scale) of the UHV system showing the primary components: (A) sample transfer translation stage, (B) load-lock chamber and pump, (C) chemical agent vapor dose manifold, (D) gate valve, (E) IR light entrance optics, (F) capillary array doser, (G) apertures and differential pumping stage, (H) mass spectrometer chamber and pump, (I) cryostat for solid sorbent doser, (J) directional agent vapor doser, (K) IR light exit optics and detector, (L) XPS system and ion gun, (M) foreline pumps for the turbomolecular pumps.

The vapor pressure of the CWAs was sufficient to allow room-temperature vapor dosing once the entire manifold volume was evacuated. Freeze–pump–thaw cycles using liquid nitrogen removed dissolved gases as well as remaining air from the manifold prior to vapor dosing. The vapor manifold line introduced CWA vapor to the UHV chamber through a precision leak valve with a directional heated tube on the UHV side to direct the vapor to the sample surface.

Uptake of the CWA was monitored in situ using RAIRS. For these data, a vacuum IR spectrometer (Vertex 80v, Bruker) has been modified to mate with the UHV system. Specifically, radiation (SiC glowbar) exits the spectrometer and is directed to a custom external optics compartment that includes a  $f = 250$  mm parabolic mirror for directing the beam through a differentially pumped KBr window and focusing it onto the surface sample. The beam size at the center of the chamber is estimated to be approximately 9 mm × 6 mm. The angle of incidence for reflection from a flat surface is 86° with respect to the sample plane. After exiting the chamber through a second differentially pumped KBr window, the diverging reflected beam is then focused with an ellipsoidal mirror ( $f_1/f_2 = 250/40$  mm) onto the sensor element of a liquid-nitrogen-cooled mercury cadmium telluride (MCT) detector. The entire beam path can be operated under vacuum, which is important for removing background gases from the spectra. In addition, the mirrors in the system are high reflectivity Au-coated mirrors to minimize loss of photons throughout the beam path.

The IR spectrum of silica is shown in Figure 6, which was collected after pretreatment of the silica at 700 K for 5 min. The spectrum shows a sharp peak at 3745  $\text{cm}^{-1}$ , which is characteristic of isolated hydroxyls. The absence of a broad feature near 3500  $\text{cm}^{-1}$  indicates the removal of most associated hydroxyls. Work by Zhuravlev<sup>6</sup> suggests that, under our annealing conditions, free hydroxyls dominate the surface, but there remain approximately 20% geminal groups. The small peak near 3000  $\text{cm}^{-1}$  wavenumbers is likely due to trace hydrocarbon contamination that could not be removed



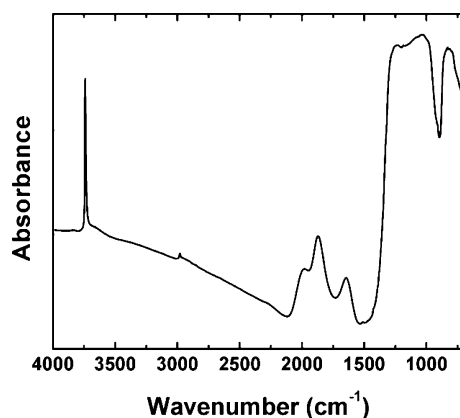


Figure 6. IR spectrum of silica after pretreatment at 700 K for 5 min.

regardless of sample annealing conditions. The intensity and position of this peak were unaffected by sarin and soman adsorption.

Although IR spectroscopy yields information about the vibrational frequencies of surface adsorbates, complete characterization of the activation energy for desorption was performed via kinetic analysis of TPD data. TPD is performed by first exposing the surface to a species of interest. During this initial exposure, RAIRS is employed to monitor surface uptake and determine coverage. Initial dosing is typically performed at low surface temperatures where residence times are sufficient to ensure constant coverage following dosing. Once dosing is complete, the chamber is evacuated to remove background gas-phase agent. The temperature of the surface is then increased by driving the sample heater with a power supply under proportional-integral-derivative control (LPS-800-1, Thermionics). With the liquid nitrogen reservoir on the sample holder filled, the temperature can be ramped at a rate of 0.5 K/s with approximately  $\pm 1$  K precision. During the thermal ramp, IR and mass spectra are recorded to track desorption from the surface. Mass spectral intensity versus surface temperature represents the rate of desorption, which is governed by the activation energy for desorption. In the absence of chemical reactions, the desorption rate curves can be analyzed to reveal properties about the activation energy for desorption.

As products are released from the surface during TPD, they are tracked with a doubly differentially pumped quadrupole mass spectrometer, (Extrel, MAX1000  $m/z = 1-1000$ ). Each differential stage is evacuated by a 450 L/s magnetically levitated turbomolecular pump (Edwards STP-451C), which enables up to 3 orders of magnitude pressure differential between the main chamber and mass spectrometer chamber during an experiment. The line-of-sight of the mass spectrometer is defined by a series of apertures that separate the differential pumping stages such that the ionizer of the mass spectrometer views a 1 cm<sup>2</sup> spot on the surface when the surface is located at the focal point of the main chamber. The acceptance angle of the spectrometer is 1° in polar and azimuthal angles. As indicated in Figure 5, the mass spectrometer is aligned such that it views the surface during dosing and while performing IR spectroscopic measurements. In this way, changes in surface vibrational modes and concentrations during dosing can be directly correlated with the mass spectra of species desorbing from the surface at any point in time. A second mass spectrometer (RGA 300M, Stanford Research Systems,  $m/z = 1-300$ ) mounted directly on

the UHV chamber provided independent confirmation of intact molecular desorption of the CWA and was used to confirm high purity of the agent as the vapor entered the chamber.

The absence of significant CWA decomposition on the silica surfaces during the experiments was corroborated by XPS data recorded following the IR/TPD experiments. The XPS instrumental component of this UHV system consists of a dual anode (Al K $\alpha$  and Mg K $\alpha$ ) X-ray source (DAR 400, Omicron Nanotechnology) and is equipped with a Z translation stage with 5° X–Y tilt for alignment with the sample. Detection of photoelectrons is achieved with an Omicron Sphera hemispherical analyzer with a five-channel detector mounted at a 45° angle relative to the X-ray source. Energy calibration was performed using the Au 4f<sub>7/2</sub> peak observed from the gold substrate at 84.00 eV. A typical XPS data set is shown in Figure 7, which was collected from a silica

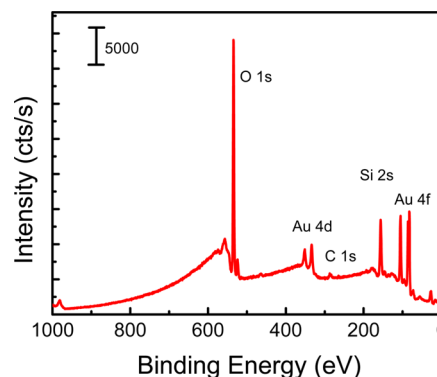


Figure 7. Survey XPS data collected after several cycles of sarin and soman exposure followed by TPD. Note the absence of P or F signal. Au is present due to the substrate supporting the silica film, and the small amount of carbon is due to trace concentrations of hydrocarbons on the silica surface.

surface after several TPD cycles using both sarin and soman. The absence of phosphorus or fluorine, which would be expected to be present on the surface of metal oxides after reacting with organophosphorus compounds,<sup>14,15</sup> confirms that desorption is molecular and does not involve significant chemical reactions.

## AUTHOR INFORMATION

### Corresponding Author

\*E-mail: jrmorris@vt.edu.

### Notes

The authors declare no competing financial interest.

## ACKNOWLEDGMENTS

The support of the Army Research Office (W911NF-09-1-0150), the Defense Threat Reduction Agency (W911NF-06-1-0111 and BB11PHM156), and the National Science Foundation (CHE-0547543) is gratefully acknowledged. The authors also acknowledge Dr. Charles Bass, Dr. Glenn Lawson, and Mr. Mark Morgan at the Defense Threat Reduction Agency in addition to Dr. Stephen Lee and Dr. Jennifer Becker at the Army Research Office for their support.

## REFERENCES

- (1) Wilmsmeyer, A. R.; Uzarski, J.; Barrie, P. J.; Morris, J. R. Interactions and Binding Energies of Dimethyl Methylphosphonate

and Dimethyl Chlorophosphate with Amorphous Silica. *Langmuir* **2012**, *28*, 10962–10967.

(2) Troya, D.; Edwards, A. C.; Morris, J. R. Theoretical Study of the Adsorption of Organophosphorus Compounds to Models of a Silica Surface. *J. Phys. Chem. C* **2013**, *117*, 14625–14634.

(3) Wilmsmeyer, A. R.; Gordon, W. O.; Davis, E. D.; Mantooth, B. A.; Lalain, T. A.; Morris, J. R. Multifunctional Ultra-High Vacuum Apparatus for Studies of the Interactions of Chemical Warfare Agents on Complex Surfaces. *Rev. Sci. Instrum.* **2014**, *85*, 014101.

(4) Legrand, A. P., Ed. *The Surface Properties of Silicas*; John Wiley & Sons: New York, 1998.

(5) Bergna, H. E.; Roberts, W. O. *Colloidal Silica: Fundamentals and Applications*; CRC Press: Boca Raton, FL, 2005.

(6) Zhuravlev, L. T. Concentration of Hydroxyl-Groups on the Surface of Amorphous Silicas. *Langmuir* **1987**, *3*, 316–318.

(7) Wilmsmeyer, A. R.; Gordon, W. O.; Davis, E. D.; Troya, D.; Mantooth, B. A.; Lalain, T. A.; Morris, J. R. Infrared Spectra and Binding Energies of Chemical Warfare Nerve Agent Simulants on the Surface of Amorphous Silica. *J. Phys. Chem. C* **2013**, *117*, 15685–15697.

(8) Taylor, D. E.; Runge, K.; Cory, M. G.; Burns, D. S.; Vasey, J. L.; Hearn, J. D.; Griffith, K.; Henley, M. V. Surface Binding of Organophosphates on Silica: Comparing Experiment and Theory. *J. Phys. Chem. C* **2013**, *117*, 2699–2708.

(9) Bermudez, V. M. Computational Study of the Adsorption of Trichlorophosphate, Dimethyl Methylphosphonate, and sarin on Amorphous SiO<sub>2</sub>. *J. Phys. Chem. C* **2007**, *111*, 9314–9323.

(10) Henderson, M. A.; Jin, T.; White, J. M. A TPD/AES Study of the Interaction of Dimethyl Methylphosphonate with  $\alpha$ -Fe<sub>2</sub>O<sub>3</sub> and SiO<sub>2</sub>. *J. Phys. Chem.* **1986**, *90*, 4607–4611.

(11) Zubkov, T.; Smith, R. S.; Engstrom, T. R.; Kay, B. D. Adsorption, Desorption, and Diffusion of Nitrogen in a Model Nanoporous Material. I. Surface Limited Desorption Kinetics in Amorphous Solid Water. *J. Chem. Phys.* **2007**, *127*, 184707.

(12) Quenneville, J.; Taylor, R. S.; van Duin, A. C. T. Reactive Molecular Dynamics Studies of DMMP Adsorption and Reactivity on Amorphous Silica Surfaces. *J. Phys. Chem. C* **2010**, *114*, 18894–18902.

(13) Badger, R. M.; Bauer, S. H. Spectroscopic Studies of the Hydrogen Bond. II. The Shift of the O–H Vibrational Frequency in the Formation of the Hydrogen Bond. *J. Chem. Phys.* **1937**, *5*, 839–851.

(14) Gordon, W. O.; Tissue, B. M.; Morris, J. R. Adsorption and Decomposition of Dimethyl Methylphosphonate on Y<sub>2</sub>O<sub>3</sub> Nanoparticles. *J. Phys. Chem. C* **2007**, *111*, 3233–3240.

(15) Chen, D. A.; Ratliff, J. S.; Hu, X.; Gordon, W. O.; Senanayake, S. D.; Mullins, D. R. Dimethyl Methylphosphonate Decomposition on Fully Oxidized and Partially Reduced Ceria Thin Films. *Surf. Sci.* **2010**, *604*, 574–587.